The ADV signal in general was disturbed but we could measure close to the bottom (see figure 8 illustrating a typical result). Although the net ADV profile data present much scatter, for the second order Stokes condition K2 a small net current in the crest direction was distinguished as well as the asymmetry induced boundary layer streaming in the opposite direction. For the wave and current condition K5 the profile was logarithmic. These findings are in accordance with previous measurements in the tunnel.

Comparison of ADV and laser measurements for K2 showed a systematic difference which is small in the time dependent values but significant when averaged over the wave period. In Katopodi et al (1994), a similar mismatch was found when comparing laser and EMF (electromagnetic flow meter) measurements for waves and currents. Although the two cases are not directly comparable, they both concern asymmetric flows (K2 second order Stokes, series E current and sinusoidal waves).

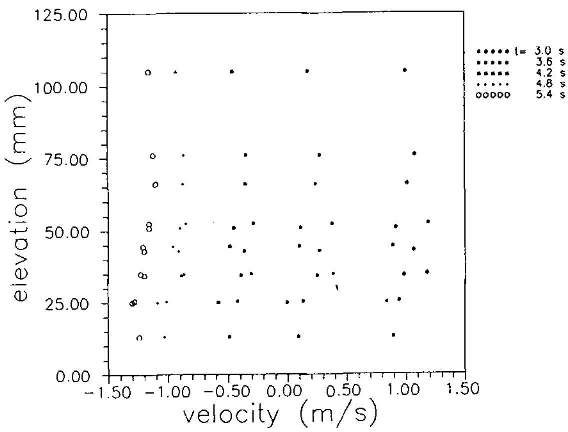

Figure 8: Time dependent velocity profiles measured by ADV test K5 between 3.0 and 5.4 secs.

Conclusions

An experimental investigation of graded sediment transport was conducted in the Large Oscillating Water Tunnel of WL | Delft Hydraulics under various hydraulic conditions with plane bed. The sediment bed consisted of a mixture of two well sorted sands (two fractions) that have been used before in the tunnel. The experiment concerned measurements of net sediment transport rates, bed composition change, time averaged suspended sediment profiles, time dependent concentrations in the suspension and sheet

This is a preview. Click here to purchase the full publication.

flow layers and time dependent velocity profiles. A detailed presentation of the measurements and results is presented in the data report (Hamm et al, 1998).
Furthermore, net transport rates per sediment fraction were calculated by Cloin (1998) based on the bed composition data.

The data set has then been used by Cloin (1998) to compare with previous experiments using uniform sands. She also used it for the experimental verification of various transport formulae as well as time dependent models of sediment transport of graded sediment in sheet-flow conditions. This work is being extended to enlighten the influence of size and density in selective transport mechanisms. The examination of the gradation characteristics of the suspended sand samples and their linking with the characteristics of the bed samples is also scheduled (Katopodi et al., 1999).

As seen from the bed composition results, the used bed sampling technique did not prove very accurate and should be improved, possibly by taking cores out of the bed or colouring one of the fractions. Moreover, it would be very useful if the measurements concerning the two well sorted sands that constitute the sediment mixture of this experiment were completed such that all the quantities measured for series K could be compared with measurements of sand consisting out of one fraction only (see Hamm et al, 1998).

Acknowledgements

The experiments were part of the project « Access to the experimental facilities of WL | DELFT HYDRAULICS in the framework of the EU programme « Training and Mobility of Researchers », contract n° ERBFMGECT950045. The analysis of the data has been performed in the framework of the SAFE project carried out as part of the MAST III programme, partly funded by the European Commission/ Directorate of Science, Research and Development (DG-XII), contract MAS3-CT95-0004 and by national bodies including Sogreah Ingénierie, Ministère de l'Equipement, des Transports et du Logement/Direction de la Recherche et des Affaires Scientifiques et Techniques/Service Technique des Ports Maritimes et des Voies Navigables (France), subvention N° 97 M/3 and the Netherlands Centre for Coastal Research (NCK).

References

Cloin, B. (1998): Gradation effects on sediment transport in oscillatory sheet-flow. M.Sc. Thesis, Delft University of Technology, Report H2305, March 1998, WL | Delft Hydraulics, The Netherlands.

This is a preview. Click here to purchase the full publication.

Dohmen-Janssen, C.M., G. van der Hout and J.S. Ribberink (1998). Phase-lag effects in oscillatory sheet flow. Proc. 26th Int. Conf. on Coastal Engng., Copenhagen, Denmark, ASCE, in press.

Hamm L., I. Katopodi, C.M. Dohmen-Janssen, J.S. Ribberink, P. Samothrakis, B. Cloin, J.C. Savioli, Y. Chatelus, J. Bosboom, J. Nicholson, R. Hein (1998): Grain Size, Gradation and Density effects on Sediment Transport Processes in Oscillatory flow conditions. Data Report Z2153, Part I: The effects of grain size gradation (Series K), WL | Delft Hydraulics, The Netherlands.

Janssen, C.M. and J.S. Ribberink (1996). Grain-size influence on sand transport in oscillatory sheet flow. Proc. 25th Int. Conf. on Coastal Engng., Orlando, FL, USA, ASCE, 4779-4792

Katopodi, I., J.S. Ribberink, P. Ruol and C. Lodahl (1994). Sediment transport measurements in combined wave-current flows. Proc. Coastal Dynamics'94 conf., Barcelona, Spain, ASCE, 837-851.

Katopodi, I., J.S. Ribberink, L. Hamm, P. Samothrakis, N. Kitou, C.M. Dohmen-Janssen and J.C. Savioli (1999). Comparison of concentrations measured in an oscillating tunnel with well-sorted and bimodal sand. Accepted for Coastal Sediments'99 Conference, Long Island, USA, ASCE.

Manso, F., R.L. Koomans, R.J. de Meijer and F. Vilas(1998). The effect of density gradation in oscillatory sediment transport. Proc. 26th Int. Conf. on Coastal Engng., Copenhagen, Denmark, ASCE, in press.

Ribberink, J.S. and A.A. Al-Salem (1994). Sediment transport in oscillatory boundary layers in cases of rippled beds and sheet-flow. J. Geophys. Res., vol.99, n°C6, 12,707-12,727

Ribberink, J.S. and A.A. Al-Salem (1995). Sheet-flow and suspension of sand in oscillatory boundary layers. Coastal Engineering, 25, 205-225.

Ribberink, J.S., I. Katopodi, K.A.H. Ramadan, R. Koelewijn and S. Longo (1994). Sediment transport under (non)-linear waves and currents. Proc. 24th Int. Conf. on Coastal Engng., Kobe, Japan, ASCE, 2527-2541.

Tánczos, I.C., de Meijer, R.J., Ribberink, J.S., Janssen, C.M. (1997). Selective transport of heavy and light minerals under asymmetric waves, Submitted to Sedimentology.

This is a preview. Click here to purchase the full publication.

Phase-lag effects in oscillatory sheet flow

C. Marjolein Dohmen-Janssen[1], Gizella van der Hout[1], Jan S. Ribberink[2]

Abstract

It is often assumed that in sheet flow conditions the transport rate in oscillatory flow behaves quasi-steady, i.e. showing a direct relation with the instantaneous flow velocity (e.g. Ribberink et al., 1994). In this paper it will be shown that this assumption is not always valid.

Therefore a new semi-unsteady sand transport model is developed which takes into account phase-lag effects of the sediment on the net transport rate. In order to verify this new semi-unsteady model and two existing quasi-steady models, new experiments were performed in the Large Oscillating Water Tunnel (LOWT) of WL | DELFT HYDRAULICS. Together with earlier experiments these measurements form a data set of net sand transport rates of uniform sand for three different grain sizes (D_{50} = 0.13; 0.21 and 0.32 mm) in combined wave-current sheet flow conditions.

The verification shows that phase-lag effects become important for a combination of fine sand, large flow velocities and small wave periods. Under these conditions the quasi-steady models cannot predict the behaviour of the net transport rates correctly and the predictions of the new semi-unsteady model show much better agreement.

Introduction

Sheet flow corresponds to conditions of high velocities when ripples are washed out and the bed becomes flat. In those conditions the majority of the sand transport takes place in a thin, high-concentrated layer close to the bed, i.e. the sheet flow layer.

Because of the small thickness of this layer it is generally assumed that the response time of the sand transport process to changes in flow conditions is small compared to the wave period. If that is the case, it can be expected that the time-dependent sediment transport rate depends directly on the instantaneous flow velocity or bed shear stress. This assumption is applied in all quasi-steady models.

[1] Delft University of Technology, Hydraulics & Offshore Eng. Section. p/a University of Twente, Section of Civil Eng. & Management, PO Box 217, 7500 AE Enschede, The Netherlands, phone: 31 53 4892831, fax 31 53 4894040, email: c.m.dohmen-janssen@sms.utwente.nl

[2] University of Twente, Section of Civil Eng. & Management, PO Box 217, 7500 AE Enschede, The Netherlands, phone: 31 53 4892767, fax 31 53 4894040, email: j.s.ribberink@sms.utwente.nl

This is a preview. Click here to purchase the full publication.

If the response time of sediment particles is not small compared to the wave period, the sediment concentration may lag behind the velocity. This will be caused by the fact that both the sediment entrainment from the bed into the flow and the settling of the particles back to the bed takes time. The latter depends on the settling time of a particle and on the height to which the particle is entrained, which is expected to be determined by the flow velocity.

Therefore it is expected that phase-lags will become important if sediment is entrained relatively high into the flow (large oscillatory velocities) and slowly settles down to the bed (fine sand) while the available fall time is short (small wave period). Moreover, it is expected that if phase-lags occur, the net transport rates are reduced. This can be explained as follows: If the transport behaves quasi-steady, the net (wave-averaged) transport rate under asymmetric oscillatory flow will always be in direction of the largest velocity, due to the non-linear relation between velocity and sand transport rate. If the sediment concentration lags behind the flow velocity, part of the sediment that is picked-up under a certain half wave cycle, may still be entrained into the flow and transported in opposite direction during the successive half wave cycle.

A new semi-unsteady model is developed to take into account the effect of phase-lags on the net transport rates. The model is called semi-unsteady, because it accounts for phase-lag effects, without describing the complete time-dependent velocity and concentration profiles. Apart from the new *semi-unsteady* model, also two existing *quasi-steady* models are presented, in order to compare the differences between these two types of models. The three transport models are verified against experimental data.

The set-up of the experiments and the measured net transport rates are presented first. Next the two existing quasi-steady models are described shortly and the new semi-unsteady model is presented. Finally, the behaviour of the measured net transport rates is discussed in relation with the predictions of the three transport models.

New experiments

Two new sets of sand transport experiments were carried out with uniform sand of different grain sizes. The experiments were performed in the Large Oscillating Water Tunnel (LOWT) at WL | DELFT HYDRAULICS from October 1996 to January 1997. The mean grain sizes of the two sands were 0.32 and 0.21 mm for series I and J respectively. The experiments are a follow up of the previous experimental series with 0.21 mm sand (Series E: Katopodi et al., 1994) and 0.13 mm sand (Series H: Janssen and Ribberink, 1996 and Janssen et al., 1997). The measurements of these four series can be considered as one consistent data set on sediment transport under combined wave-current flow in the sheet flow regime.

The LOWT of WL | DELFT HYDRAULICS is a large-scale facility that allows experiments to be performed at full scale (1:1). It consists of a large U-shaped tube, with a long horizontal test section and two vertical cylindrical risers. One of them is open to the air; the other riser contains a steel piston. The piston sets the water in motion and induces an oscillating water motion in the test section. The test section is 14 m long, 0.3 m wide and 1.1 m high. A 0.3 m thick sand bed can be brought into the test section, leaving 0.8 m for the oscillating water flow above the bed.

This is a preview. Click here to purchase the full publication.

Underneath both risers a sand trap is constructed. The range of oscillatory velocities is 0.2-1.8 m/s; the range of periods is 4-15 s.

A recirculation flow system for the generation of a net current is connected to both cylindrical risers. The maximum superimposed net current velocity in the test section is about 0.5 m/s. A third sand trap is constructed in this recirculation system. A picture of the LOWT is given in Figure 1.

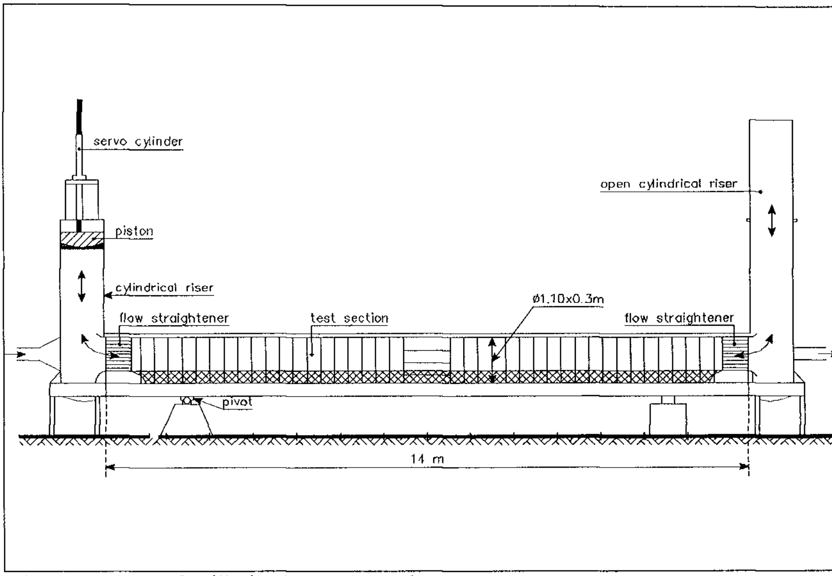

Figure 1: Large Oscillating Water Tunnel

The characteristics of the three sands, used in the experimental series are:

Series H:	$D_{10} = 0.10$ mm,	$D_{50} = 0.13$ mm,	$D_{90} = 0.18$ mm
Series E/J:	$D_{10} = 0.15$ mm,	$D_{50} = 0.21$ mm,	$D_{90} = 0.32$ mm
Series I:	$D_{10} = 0.22$ mm,	$D_{50} = 0.32$ mm,	$D_{90} = 0.46$ mm

The test conditions consisted of different combinations of a sinusoidal oscillatory flow and a net current. A condition is characterised by the wave period T (s), the velocity amplitude u_a (m/s) and the mean current velocity u_m (m/s) measured at 10 cm above the bed. For the present series I and J the conditions are mainly the same as in the previous experimental series with unsieved dune sand with D_{50}= 0.21 mm (Series E) and fine sand with D_{50}= 0.13 mm (Series H).

For every condition net (wave-averaged) transport rates were measured, together with the flow velocity at 10 cm above the bed. Net transport rates were derived from measured bed level changes and the weight of the sand, collected in the traps.

The measured net transport rates are based on measurements over the full width of the tunnel. However, the velocities are measured in the centreline of the tunnel. Due to boundary layer effects the net current velocities in the centreline are somewhat

This is a preview. Click here to purchase the full publication.

higher than the width-averaged values. Therefore the net transport rates are corrected such that they correspond to the measured velocities in the centreline of the tunnel (see e.g. Van der Hout, 1997). Table 1 presents the measured wave periods and flow velocities, together with the corresponding net transport rates, expressed in m^2/s, i.e. volume of sand per unit width per second.

Table 1: Measured wave periods, flow velocities and net transport rates

Test	D_{50} (mm)	T (s)	u_a (m/s)	u_m (m/s)	$\langle q_s \rangle$ (10^{-6} m^2/s)
H2	0.13	7.2	0.68	0.23	18.8
H3	0.13	7.2	0.93	0.24	34.9
H4	0.13	7.2	1.09	0.25	40.0
H5	0.13	7.2	1.30	0.24	51.7
H6	0.13	7.2	1.47	0.24	65.5
H7	0.13	7.2	0.49	0.42	15.6
H8	0.13	7.2	0.67	0.43	47.4
H9	0.13	7.2	0.94	0.43	85.7
H24	0.13	4.0	0.68	0.24	12.8
H44	0.13	4.0	1.06	0.25	9.0
H212	0.13	12.0	0.68	0.23	19.9
H412	0.13	12.0	1.09	0.24	97.1
J1	0.21	7.20	1.06	0.24	46.3
J2	0.21	7.20	1.28	0.25	74.4
E2	0.21	7.22	1.47	0.23	111.8
J3	0.21	7.20	0.46	0.41	9.0
J4	0.21	7.20	0.65	0.41	25.3
E4	0.21	7.23	0.95	0.44	84.4
J5	0.21	4.00	1.04	0.24	29.2
J6	0.21	12.0	1.09	0.23	49.2
I1	0.32	7.2	1.47	0.26	94.0
I2	0.32	7.2	1.70	0.25	152.3
I3	0.32	7.2	0.65	0.42	23.6
I4	0.32	7.2	0.92	0.42	53.3
I5	0.32	7.2	1.50	0.45	193.7

This is a preview. Click here to purchase the full publication.

For conditions E1–E4, H6, H9, and I1 also time-dependent measurements were carried out: During the wave cycle both flow velocities and sediment concentrations at different levels above the sand bed were measured. Moreover, video recording were taken to determine the bed level variation during the wave cycle. These time-dependent measurements are not included in this paper (see e.g. Katopodi et al., 1994; Ribberink et al. 1994; Janssen et al., 1997 and Janssen and Van der Hout, 1997).

Quasi-steady model of Bailard (1981)

Bailard applied the theoretical energy consideration of Bagnold (1963) to determine the sand transport rate. He assumed that the sediment transport rate is proportional to the available fluid power, which is equal to the work done by the fluid, i.e. the absolute value of the fluid shear stress times the velocity.

The model consists of a bed load and a suspended load component. Each component includes a term that depends on the bed slope. The bed slope terms are not included here, because the sand bed in the experiments is horizontal. The equation reads:

$$q_s(t) = \frac{c_f}{(s-1)\,g}\left(\frac{\varepsilon_b u^3(t)}{\tan\varphi} + \frac{\varepsilon_s \left|u^3(t)\right| u(t)}{w_{fall}}\right) \tag{1}$$

Here q_s is the sediment transport rate, t is time, c_f is a friction factor, s is the relative density ($s = \rho_s/\rho$ with ρ_s the density of the sediment and ρ the density of water), g is the gravity acceleration, u is the horizontal velocity, φ is the angle of internal friction and w_{fall} is the fall velocity. The coefficients ε_b (= 0.1) and ε_s (= 0.02) are efficiency factors for the bed load and the suspended load transport.

In the present study the friction factor is calculated as a combined wave-current friction factor, as described by Ribberink (1998). The bed roughness height is considered to be equal to the grain diameter, i.e. $k_s = D_{50}$.

Quasi-steady model of Ribberink (1998)

The quasi-steady model of Ribberink is a bed load model. However, Ribberink considers all transport in the sheet flow layer as bed load. In sheet flow conditions the majority of the transport is transported inside the sheet flow layer, which means that the total transport will only be slightly larger than the bed load component, defined in this way.

Ribberink assumed the sand transport rate to be proportional to the difference between the actual time-dependent bed shear stress and the critical bed shear stress. The bed shear stress is expressed in terms of the (dimensionless) Shields parameter:

$$\theta(t) = \frac{\tau_b(t)}{\rho(s-1)\,g D_{50}} \tag{2}$$

Here τ_b is the time-dependent bed shear stress and D_{50} is the mean grain diameter. The sand transport rate is normalised by the parameter $\sqrt{(s-1)\,g D_{50}^3}$. This gives the following expression for the sand transport rate:

$$q_s(t) = m\sqrt{(s-1)gD_{50}^3}\,\left(\left|\theta(t)\right| - \theta_{cr}\right)^n \frac{\theta(t)}{\left|\theta(t)\right|} \tag{3}$$

The values of the coefficients m and n are based on many data from laboratory and field experiments with steady and oscillatory flows: m = 11, n = 1.65.

This is a preview. Click here to purchase the full publication.

New semi-unsteady model

As mentioned in the introduction, phase-lag effects are expected for fine sand, large oscillatory velocities and small wave periods. Moreover, phase-lag effects are expected to reduce the net transport rate. Therefore a new-semi unsteady model is developed which predicts the same net transport rates as the quasi-steady model of Ribberink if phase-lag effects are small and smaller net transport rates if phase-lag effects become important.

This is realised by introducing a correction factor r to the calculated net transport rates of the model of Ribberink. The correction factor r is equal to 1.0 if no phase-lag effects occur and decreases for increasing phase-lag effects.

The correction factor r is defined as the ratio of the net sand transport rate, including phase-lag effects (*real* net transport rate) to the net sand transport rate when phase-lag effects are neglected (*equilibrium* net transport rate). These transport rates are calculated as follows:

$$q_s(t) = \int_0^h u_\infty(t) * c(z,t)\, dz \qquad (4)$$

Here h is the water depth, $u_\infty(t)$ is the periodic velocity outside the wave boundary layer, (free-stream velocity) and c is the sediment concentration. The time-dependent sediment concentration profile c(z,t) is derived from an advection-diffusion equation. Nielsen (1979) showed that this equation can be solved analytically if a constant sediment mixing coefficient ε_s is used. The advection-diffusion equation reads:

$$\frac{\partial c}{\partial t} = \frac{\partial}{\partial z}\left[w_{fall} c + \varepsilon_s \frac{\partial c}{\partial z} \right] \qquad (5)$$

The *equilibrium* sand transport rate is equal to the product of the free-stream velocity and the equilibrium concentration profile, while the *real* sand transport rate is equal to the product of the free-stream velocity and the real concentration profile.

To derive the time-dependent *equilibrium* concentration profile, it is assumed that thc concentration profile adjusts itself instantaneously to changes in flow velocity. This corresponds to a solution of the advection-diffusion equation for which the term $\partial c/\partial t$ is set zero. The time-dependent *real* concentration profile is derived without this assumption, which corresponds to the solution of the complete advection-diffusion equation, i.e. including the term $\partial c/\partial t$.

The bottom boundary condition for the equilibrium concentration profiles is based on the assumption that thc bottom concentration is instantaneously related to the flow velocity. Using a coefficient a and exponent b this can be expressed as follows:

$$c(0,t) = a\left| u(t)^b \right| \qquad (6)$$

For the real concentration profiles the bottom boundary condition is based on the assumption that the *pick-up rate* of sediment is directly related to the instantaneously velocity. This implies that the concentration *gradient* is instantaneously related to the flow velocity:

This is a preview. Click here to purchase the full publication.

$$\left.\frac{\partial c}{\partial z}\right|_{z=0} = -\frac{w_{fall}}{\varepsilon_s} a \left| u(t)^b \right| \tag{7}$$

The advection-diffusion equation only has an analytical solution if b is even. In the present study b = 2 is chosen, giving a transport rate proportional to u^3. This is close to the value of 3.3 in the model of Ribberink (1998), which results for negligible values of the critical Shields parameter, as is the case in sheet flow conditions.

Applying all these considerations results in the following expressions for the real and the equilibrium sand transport rate, i.e. $q_{s,r}$ and $q_{s,eq}$, respectively:

$$q_{s,r}(t) = \left[\sum_{k=0}^{N} u_k \cos(k\omega t)\right] \left[\sum_{k=0}^{2N} \frac{\varepsilon_s}{w_{fall}} \frac{\hat{c}_{bk}}{\left(P_k^2 + Q_k^2\right)^{\frac{3}{2}}} \left[P_k \cos(k\omega t + \varphi_k) + Q_k \sin(k\omega t + \varphi_k)\right]\right] \tag{8}$$

$$q_{s,eq}(t) = \left[\sum_{k=0}^{N} u_k \cos(k\omega t)\right] \left[\sum_{k=0}^{2N} \frac{\varepsilon_s}{w_{fall}} \hat{c}_{bk} \cos(k\omega t)\right] \tag{9}$$

With:

$$\hat{c}_{b0} = a\left(u_0^2 + \tfrac{1}{2}u_1^2\right) \tag{10}$$

$$\hat{c}_{b1} = a\left(2u_1u_0\right) \tag{11}$$

$$\hat{c}_{b2} = a\left(\tfrac{1}{2}u_1^2\right) \tag{12}$$

$$P_k = \frac{1}{2} + \left[\frac{1}{16} + \left(\frac{k\varepsilon_s\omega}{w_{fall}^2}\right)^2\right]^{\frac{1}{4}} \cos\left(\tfrac{1}{2}\alpha_k\right) \tag{13}$$

$$Q_k = \left[\frac{1}{16} + \left(\frac{k\varepsilon_s\omega}{w_{fall}^2}\right)^2\right]^{\frac{1}{4}} \sin\left(\tfrac{1}{2}\alpha_k\right) \tag{14}$$

$$\alpha_k = \arctan\left(\frac{4k\varepsilon_s\omega}{w_{fall}^2}\right) \tag{15}$$

$$\varphi_k = \arctan\left(-\frac{Q_k}{P_k}\right) \tag{16}$$

Here ω is the angular frequency of the wave (= $2\pi/T$, with T the wave period) and u_k is the k^{th} harmonic of the horizontal velocity. In the present analysis only u_0 and u_1 are considered (sinusoidal oscillatory flow plus a net current), because all experimental conditions consist of sinusoidal oscillatory flow combined with a net current.

As mentioned before, the correction factor r is defined as the ratio of thc *net* real sand transport rate to the *net* equilibrium sand transport rate. These net sand transport rates can be determined by averaging Eqs.(8) and (9) over time.

From these cquations it can be seen that the difference between the equilibrium and the real transport rate (and thus the value of the correction factor) is fully detcrmined by $\varepsilon_s\omega/w^2_{fall}$, called the phase-lag parameter p. The ratio of sediment mixing coefficient to fall velocity ε_s/w_{fall} can be considered as a characteristic length δ to which particles are entrained. Therefore the phase-lag parameter can be written as:

This is a preview. Click here to purchase the full publication.